

Monastrol Targeted *KIF11* Showed Potential Treatment Effective of Small Cell Lung Cancer

Xiaye Lv^{1*}, Xinhui Wang², Pengcheng Zhou³, Shanshan Jiang⁴, Baolin Zhou⁵, Haoqun Xie⁶, Bo Yu⁶, Yuanyuan Hou⁶

¹Department of Hematology and Oncology, Honghui Hospital, Xi'an Jiaotong University, Xian, China; ²Department of Oncology, First People's Hospital of Xinxiang and The Fifth Affiliated Hospital of Xinxiang Medical College, Street Yiheng 63, Xinxiang, China; ³Department of Orthopaedics, The First Hospital of Jilin University, Street Xinmin 71, Changchun, China; ⁴Department of Zoology, China Academy of Science, Beichen West Road No.1 Courtyard, Chaoyang District, Beijing, China; ⁵Department of Gastroenterology, The First Affiliated Hospital of Xinxiang Medical College, Street Jiankang 88, Xinxiang, China; ⁶Department of Clinical, Clinical College, Jilin University, Street Xinmin 126, Changchun, China

ABSTRACT

Object: This study is to identify Small Cell Lung Cancer (SCLC) driver genes, annotate enrichment functions and key pathways, and also verify Monastrol therapeutic effect.

Methods: The gene expression profiles of GSE40275 and GSE43346 was analyzed to identify the DEGs (Differentially Expressed Genes) between SCLC and the normal tissue. GO (Gene Ontology), KEGG (Kyoto Encyclopedia of Genes and Genomes) analysis and PPI (Protein-Protein Interaction) network analysis were conducted to find out the enrichment functions, pathways and hub genes. Moreover, *in vitro*, MTT assay, colony-forming assay, and the scratch assay were performed to verify the effect of Monastrol.

Results: There were common 129 up-regulated and 176 down-regulated DEG's between SCLC samples and normal lung samples. *KIF11*, *NDC80*, and *PBK* were identified as hub genes after PPI network analysis. The q-PCR results showed that genes *KIF11*, *NDC80* and *PBK* consistently expressed higher in cancer cells than in normal cell lines. An *in vitro* assay showed that Monastrol inhibited SCLC cellular viability, proliferation and migration ($P < 0.01$).

Conclusion: *KIF11*, *NDC80* and *PBK* were aberrantly expressed and could be potentially applied as diagnostic biomarkers, therapeutic targets and prognostic biomarkers. Monastrol was a promising drug in the treatment of SCLC patients.

Keywords: Bioinformatics; Lung science; SCLC; Monastrol

INTRODUCTION

Lung cancer, one of the leading causes of cancer-related deaths worldwide, is the most common type of cancer in men and the fourth most common in women [1]. Small Cell Lung Cancer (SCLC) with a high degree of malignancy and high mortality is account for about 13%-20% of all lung cancer cases. In developed countries such as the United States, SCLC is estimated to represent about 16% of new lung cancer diagnoses, which means that about 35,000 new cases occur annually [2]. In under developed countries, the percentage of SCLC cases is higher. More than 130,000 new diagnoses of SCLC and 100,000 deaths from this disease were estimated to have occurred in China in 2013 Small cell cancer is

highly aggressive [3]. This kind of tumor cell is characterized by rapid doubling time and is not suitable for traditional surgical therapy but is sensitive to both chemotherapy and radiation. Unfortunately, these conventional treatment methods are both short and not curative in most cases with an average 5-year survival rate below 7%. No major treatment advances have occurred over the past 30 years [4]. In patients with the extensive-stage disease, chemotherapy alone can palliate symptoms and prolong survival in most patients; however, long-term survival is rare [5]. The management of SCLC is still a very challenging cause of disease outcome has remained stubbornly poor due mainly to limited options for effective treatment. Although according to some preclinical studies about the understanding of SCLC, the c-kit inhibitor

Correspondence to: Xiaye Lv, Department of Hematology and Oncology, Honghui Hospital, Xi'an Jiaotong University, Xian, China, E-mail: lxyajxc@foxmail.com

Received: 02-May-2022, Manuscript No. IMT-22-17620; **Editor assigned:** 05-May-2022, Pre QC No. IMT-22-17620 (PQ); **Reviewed:** 20-May-2022, QC No. IMT-22-17620; **Revised:** 26-May-2022, Manuscript No. IMT-22-17620 (R); **Published:** 06-Jun-2022, DOI: 10.35248/2471-9552.22.8.195.

Citation: Lv X, Wang X, Zhou P, Jiang S, Zhou B, Xie H, et al. (2022) Monastrol Targeted *KIF11* Showed Potential Treatment Effective of Small Cell Lung Cancer. *Immunotherapy*. 8:195.

Copyright: © 2022 Lv X, et al. This is an open-access article distributed under the terms of the Creative Commons Attribution License, which permits unrestricted use, distribution, and reproduction in any medium, provided the original author and source are credited.

and other agents targeting angiogenesis could show inhibition on it, the results of the actual use were somewhat disappointing and unexpected. Meanwhile, there is no clear expatriation of the neoplastic processes of SCLC [6]. In this way, conducting such a study that comprehensively depicts the molecular pathogenesis of SCLC development as well as identifies novel therapeutic agents is necessary and crucial. Monastrol, a potent and cell-permeable inhibitor targeted *KIF11* with an IC50 value of 14 μM , which causes aberrant interactions with the microtubule, and reversals at the ATP hydrolysis step, might have anti-SCLC therapeutic effects [7].

The hallmarks of cancer are the most crucial to the development of SCLC, including genomic instability and mutations, evading growth suppressors, resisting cell deaths, sustaining proliferative signaling and enabling replicative immortality. The genomic instability of SCLC is higher than in most cancers. SCLC has a mutation rate of 5.6 to 7.4 mutations per Mb, and about 175 mutations per tumor. However, few specific driver genes have been proved related to SCLC pathogenesis. To further clarify the molecular pathogenesis of this tumor, our study also used bioinformatics methods combined with GO, KEGG analysis and PPI network analysis, employing mRNA microarray datasets to screen out the hub genes and key pathways associated with SCLC.

MATERIALS AND METHODS

Microarray data

The gene expression profiles of GSE40275 and GSE43346 were collected from the GEO database (The Gene Expression Omnibus, <http://www.ncbi.nlm.nih.gov/geo>). These profiles contained 40 SCLC samples and 44 normal samples totally.

Identification of DEGs

The analysis was conducted based on raw data using the software Gene spring (version 11.5, Agilent, USA). The category of the mRNA expression data was realized with hierarchical clustering analysis. The probe quality control in Gene spring was limited by Principal Component Analysis (PCA), and probes with intensity values below the 20th percentile were filtered out using the “filter probe sets by expression” option. Then, the DEGs were identified using a classical t-test with a P-value cutoff of <0.05 and a change >2 fold, which was applied for statistically significant definition. At last, the Venn plot analysis regarding DEGs was conducted (<http://bioinformatics.psb.ugent.be/webtools/Venn/>).

Gene ontology and pathway enrichment analysis of DEGs

The DAVID database (Database for Annotation, Visualization and Intergrated Discovery, <http://david.abcc.ncifcrf.gov/>), provided a comprehensive set of functional annotation tools to understand the biological meaning underlying plenty of genes. GO (Gene Ontology) was a useful method for analyzing biological processes, molecular function and cell components of genes and KEGG (Kyoto Encyclopedia of Genes and Genomes) was a base for gene function analysis and genomic information link. In this study, GO and KEGG pathway enrichment analyses were performed using DAVID for DEG's functions analysis.

PPI network construction and modules selection

STRING (Search Tool for Retrieval of Interacting Genes, <http://string.embl.de/>) can provide PPI (Protein-Protein Interaction) analysis for bioinformatics studies. Then, the software Cytoscape was applied to screen hub genes and modules with MCODE (Molecular Complex Detection). Moreover, the function and pathway enrichment analysis of DEGs in modules were performed.

string.embl.de/) can provide PPI (Protein-Protein Interaction) analysis for bioinformatics studies. Then, the software Cytoscape was applied to screen hub genes and modules with MCODE (Molecular Complex Detection). Moreover, the function and pathway enrichment analysis of DEGs in modules were performed.

Cell lines and reagents

Human normal pulmonary epithelial cells (BEAS-2B), human normal embryonic lung fibroblast cells (MRC5), human small cell lung cancer cells (H446) and human lung adenocarcinoma cells (A549) were purchased from the ATCC (American Type Culture Collection). Those cell lines were cultured in Dulbecco's Modified Eagle's Medium (DMEM, Hyclone, USA) supplemented with 10% fetal bovine serum (FBS, Gibco, USA). These cells were cultivated in 5% CO₂ and 95% air at 37°C. And Monastrol, the small molecule inhibitor, was purchased from Apexbio Inc. (Apexbio, Houston, USA).

Real-time quantitative reverse transcription PCR

Aim to confirm the expression of hub genes in SCLC cell lines and normal human pneumocytes, we performed qRT-PCR using FastStart Universal SYBR Green Master (ROX) (Roche Diagnostics) in a CFX96 Real-Time System (Bio-Rad) according to the manufacturer's instructions and expression levels were normalized to glyceraldehyde-3-phosphate dehydrogenase (GAPDH). The 2^{- $\Delta\Delta$ Ct} method was used for qRT-PCR data analysis.

MTT assay

The cancer cells (H446, A549) and normal cells (BEAS-2B, MRC5) were plated into 96-well culture plate with a density of 500 cells/well and were treated with different doses of Monastrol respectively. The MTT reagent (Sigma) was dissolved in PBS (5 mg/ml) to measure the viability of cells. On the day of measurement, the medium was replaced with fresh DMEM supplemented with 10% FBS and diluted MTT (1:10, 10% MTT), and incubated for 3, 5 hours at 37°C. Then, the incubation medium was removed and formazan crystals were dissolved in a 200 μl solution of DMSO. The ELx800 absorbance microplate reader (BioTek Instruments, VT, USA) was applied to quantify the MTT reduction by measuring the light absorbance at 570 nm. Each test was repeated 3 times.

Colony-forming assay

The cancer cells (H446, A549) were cultured in Petri dishes with 50 cells/cm². After 24 hours, those cells were treated with different doses of Monastrol respectively. After ten days *in vitro* growth, colonies were counted. Then, colonies were rinsed with PBS, fixed in 4% paraformaldehyde, stained with 5% crystal violet for half an hour, and rinsed twice with water.

In vitro scratch assay

The H446 and A549 cells were cultured on 24-well PermanoxTM plates. A 1 ml pipette tip across each well was used to create a consistent cell-free area. The loose cells were washed out gently using DMEM. Then, the cells were exposed to different doses of Monastrol. After the scratch and at 0, 12, 24 hours, the images of the scraped area were captured with phase-contrast microscopy. The remaining wounded area and the scratch width at six different points per image were measured.

Western blotting

The H446 and A549 cells were planted at a density of 2 10⁵ cells per well in six-well plates and treated with different doses of Monastrol. Total proteins were extracted and electrophoretically separated after 48 hours. The proteins were transferred to membranes, which were subsequently incubated with secondary antibodies after being treated with primary antibodies against *KIF11* and β -actin. The membranes were visualized with an enhanced chemiluminescence detection system (Pierce; Thermo Fisher Scientific, Inc.).

Statistical analysis

All statistic data were entered into SPSS 20.0 (SPSS Inc., Chicago, Illinois, USA) for analysis. Independent-samples t-test was conducted to analyze quantitative data. P values < 0.05 were set as significance level.

RESULTS

Identification of DEGs and gene function analysis

The gene expression level of GSE40275 and GSE43346 were shown in the volcano plots (Figure 1A). Altogether 305 DEGs were picked up between normal and SCLC mRNA expression samples shown in the VENN plots (Figure 1B). The mutual DEGs were uploaded to DAVID respectively, to identify the further insight into those genes. The detailed results of GO and KEGG pathway analysis were shown in Table 1 and Figure 1C. The GO and KEGG analysis results revealed that the mutual up-regulated DEGs were mainly associated with cell division, nucleoplasm, protein binding, and Cell cycle. Meanwhile, for the mutual down-regulated DEGs, the GO and KEGG analysis results primarily enriched in immune response, plasma membrane, scavenger receptor activity, and Complement and coagulation cascades.

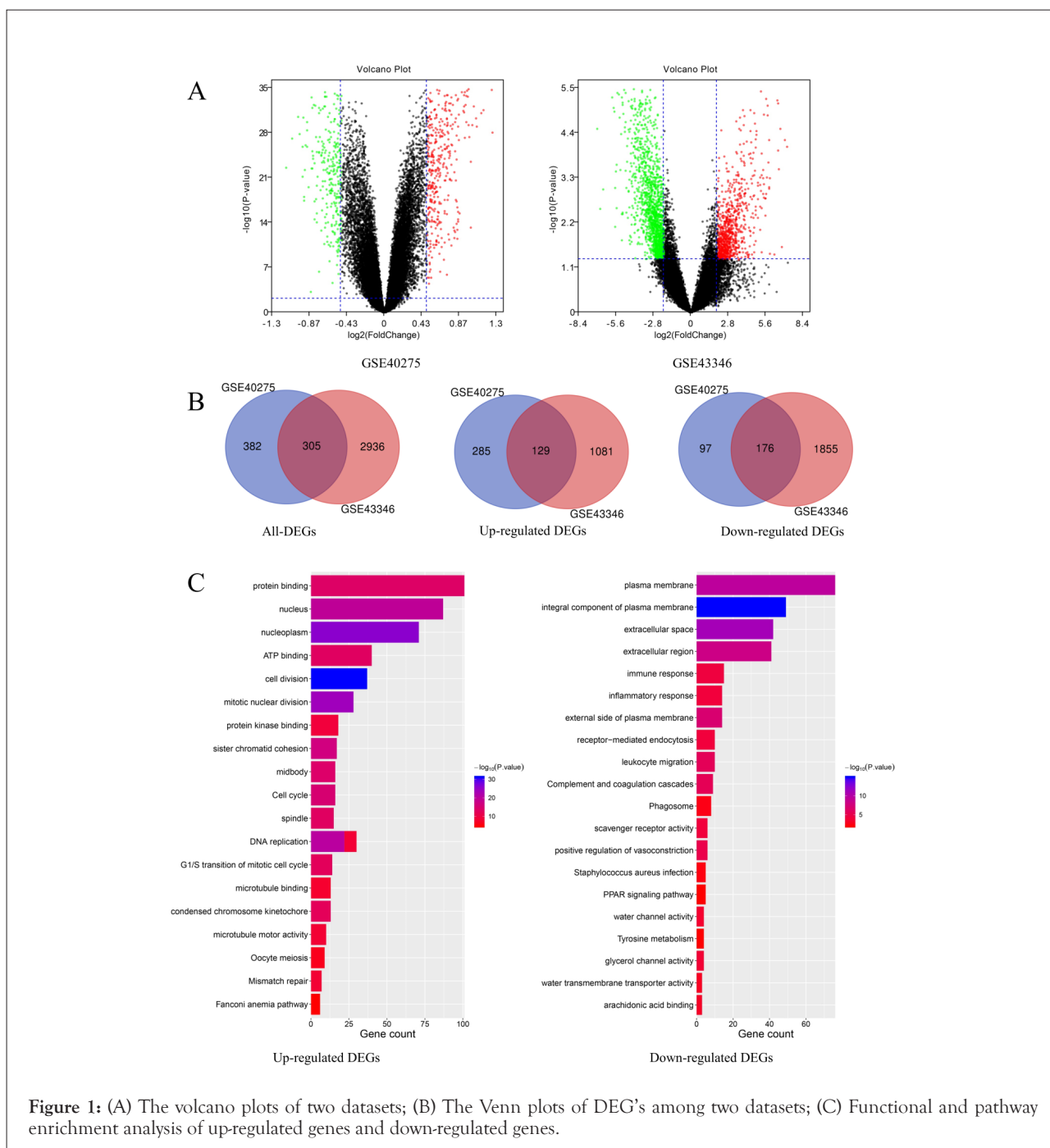


Figure 1: (A) The volcano plots of two datasets; (B) The Venn plots of DEG's among two datasets; (C) Functional and pathway enrichment analysis of up-regulated genes and down-regulated genes.

Table 1: Functional and pathway enrichment analysis of DEG's in SCLC.

Gene symbol	Degree	Between ness	Gene symbol	Degree	Between ness
<i>TOP2A</i>	112	0.11660323	<i>AURKA</i>	95	0.00363657
<i>BUB1</i>	103	0.01249734	<i>MELK</i>	95	0.0102998
<i>CCNB1</i>	103	0.01055831	<i>RFC4</i>	94	0.0142881
<i>CCNA2</i>	99	0.00526077	<i>PBK</i>	94	0.00957059
<i>KIF11</i>	99	0.00331167	<i>BUB1B</i>	93	0.00216013
<i>NDC80</i>	98	0.00388508	<i>CDKN3</i>	93	0.03636562
<i>TTK</i>	98	0.00316118	<i>CDC6</i>	92	0.0049405
<i>CHEK1</i>	97	0.00509206	<i>CCNB2</i>	92	0.00226211
<i>NCAPG</i>	96	0.00241139	<i>DTL</i>	92	0.00224199
<i>ASPM</i>	96	0.00537039	<i>RACGAP1</i>	91	0.00170142

Module screening from the PPI network

All DEGs among these samples were analyzed with a PPI network, and the hub genes were screened with degrees > 90 based on the STRING database. The top 20 genes were identified as hub genes listed in Table 2. And heat maps of these hub genes expressions were shown in Figure 2. Among those genes, the node degree of *TOP2A* was the highest one, and which degree were 112. Moreover, after MCODE analysis, the top 3 significant modules were obtained, showed in Figure 3. The functional annotation and enrichment of these modules were also performed, showed in Table 3. Enriched function analysis revealed that genes in module 1 were primarily related to protein binding, cell division and cell cycle. In modules 2-3, genes were mainly enriched in the inflammatory response, Chemokine signaling pathway, and cellular defense response.

Validation of common hub genes by qRT-PCR

To validate the expression of *KIF11*, *NDC80*, *PBK*, and *TOP2A* in human normal lung cells (BEAS-2B, MRC5), human small cell lung cancer cells (H446), and human lung adenocarcinoma cells (A549), qRT-PCR was performed. The results shown in Figure 4A revealed among those cell lines that genes *KIF11*, *NDC80*, *PBK*, and *TOP2A* were consistently expressed higher in cancer cells than in normal cell lines ($P < 0.05$).

Monastrol reduces the proliferation of SCLC cells

To evaluate the sensitivity of lung cancer cells to Monastrol, the survival cells after treatment were calculated by MTT assay. As shown in Figure 4B, following the augment of drug concentrations,

the cellular viability (ratio to control) in cell lines H446 and A549 decreased significantly. However, BEAS-2B and MRC5 still had high cellular viability even subjected to the highest dose. Monastrol was relatively tolerated for normal lung cells lines. To determine the anti-cancer effects of Monastrol in SCLC cells, we performed a colony-forming assay. The results showed us that less and smaller clonogenicities in Petri dishes with Monastrol than that in the control group (Figure 4C). The percentage of clone formation in control was significantly higher than in drug groups (0.25 $\mu\text{mol/L}$, 1 $\mu\text{mol/L}$).

Monastrol inhibits the migration of SCLC cells

The widths of scratched areas were measured after the scratch, after 12 h, and after 24 h, to research the migration of SCLC cells. In Figure 4D, the width of the scratch was significantly smaller after 24 h in the control group. However, there was only a slight decrease in the Monastrol group. In addition, after 24 h, the wounds in the control group were also smaller than in the drug group significantly. Monastrol reduces *KIF11* expression in SCLC cells.

Monastrol suppresses the expression of *KIF11* in SCLC cells

We used Western blotting to confirm that the effects of Monastrol were caused by its suppression of *KIF11* in SCLC cells. The expression of *KIF11* reduced as Monastrol concentrations increased, according to Western blotting (Figures 5A and 5B). These data suggested that Monastrol inhibits *KIF11* and thereby promotes apoptosis in SCLC cells.

Table 2: Top 20 hub genes which were screened with a degree of more than 90.

Functional and pathway enrichment analysis of DEGs in SCLC					
Expression	Category	Term	Count	%	P-value
Up-regulated	GOTERM_BP_DIRECT	GO:0051301 ~ Cell division	37	28.91	7.54E-32
	GOTERM_BP_DIRECT	GO:0007067 ~ Mitotic nuclear division	28	21.88	1.72E-24
	GOTERM_BP_DIRECT	GO:0006260 ~ DNA replication	22	17.19	3.46E-21
	GOTERM_BP_DIRECT	GO:0007062 ~ Sister chromatid cohesion	17	13.28	2.45E-17
	GOTERM_BP_DIRECT	GO:0000082 ~ G1/S transition of mitotic cell cycle	14	10.94	3.99E-13
	GOTERM_CC_DIRECT	GO:0005654 ~ Nucleoplasm	71	55.47	1.59E-26
	GOTERM_CC_DIRECT	GO:0005634 ~ Nucleus	87	67.97	2.70E-20
	GOTERM_CC_DIRECT	GO:0030496 ~ Midbody	16	12.5	8.93E-15
	GOTERM_CC_DIRECT	GO:0005819 ~ Spindle	15	11.72	7.88E-14
	GOTERM_CC_DIRECT	GO:0000777 ~ Condensed chromosome kinetochore	13	10.16	5.98E-13
	GOTERM_MF_DIRECT	GO:0005515 ~ Protein binding	101	78.91	1.97E-14
	GOTERM_MF_DIRECT	GO:0005524 ~ ATP binding	40	31.25	9.95E-14
	GOTERM_MF_DIRECT	GO:0019901 ~ Protein kinase binding	18	14.06	8.97E-10
	GOTERM_MF_DIRECT	GO:0003777 ~ Microtubule motor activity	10	7.81	4.15E-09
	GOTERM_MF_DIRECT	GO:0008017 ~ Microtubule binding	13	10.16	2.20E-08
	KEGG_PATHWAY	hsa04110: Cell cycle	16	12.5	9.02E-16
	KEGG_PATHWAY	hsa03030: DNA replication	8	6.25	2.68E-09
	KEGG_PATHWAY	hsa03430: Mismatch repair	7	5.47	5.91E-09
	KEGG_PATHWAY	hsa04114: Oocyte meiosis	9	7.03	5.59E-07
	KEGG_PATHWAY	hsa03460: Fanconi anemia pathway	6	4.69	2.42E-05
Down-regulated	GOTERM_BP_DIRECT	GO:0050900 ~ Leukocyte migration	10	5.85	2.52E-06
	GOTERM_BP_DIRECT	GO:0045907 ~ Positive regulation of vasoconstriction	6	3.51	1.21E-05
	GOTERM_BP_DIRECT	GO:0006955 ~ Immune response	15	8.77	5.17E-05
	GOTERM_BP_DIRECT	GO:0006954 ~ Inflammatory response	14	8.19	7.07E-05
	GOTERM_BP_DIRECT	GO:0006898 ~ Receptor-mediated endocytosis	10	5.85	7.42E-05
	GOTERM_CC_DIRECT	GO:0005887 ~ Integral component of plasma membrane	49	28.65	1.26E-15
	GOTERM_CC_DIRECT	GO:0005615 ~ Extracellular space	42	24.56	8.63E-12
	GOTERM_CC_DIRECT	GO:0005886 ~ Plasma membrane	76	44.44	3.59E-10
	GOTERM_CC_DIRECT	GO:0005576 ~ Extracellular region	41	23.98	6.74E-09
	GOTERM_CC_DIRECT	GO:0009897 ~ External side of plasma membrane	14	8.19	1.04E-07
	GOTERM_MF_DIRECT	GO:0005044 ~ Scavenger receptor activity	6	3.51	7.16E-05
	GOTERM_MF_DIRECT	GO:0015254 ~ Glycerol channel activity	4	2.34	1.51E-04
	GOTERM_MF_DIRECT	GO:0015250 ~ Water channel activity	4	2.34	3.75E-04
	GOTERM_MF_DIRECT	GO:0050544 ~ Arachidonic acid binding	3	1.75	8.02E-04
	GOTERM_MF_DIRECT	GO:0005372 ~ Water trans membrane transporter activity	3	1.75	0.0011953
	KEGG_PATHWAY	hsa04610: Complement and coagulation cascades	9	5.26	2.73E-06
	KEGG_PATHWAY	hsa04145: Phagosome	8	4.68	0.0033576
	KEGG_PATHWAY	hsa05150: Staphylococcus aureus infection	5	2.92	0.00526332
	KEGG_PATHWAY	hsa00350: Tyrosine metabolism	4	2.34	0.01047714
	KEGG_PATHWAY	hsa03320: PPAR signaling pathway	5	2.92	0.0112204

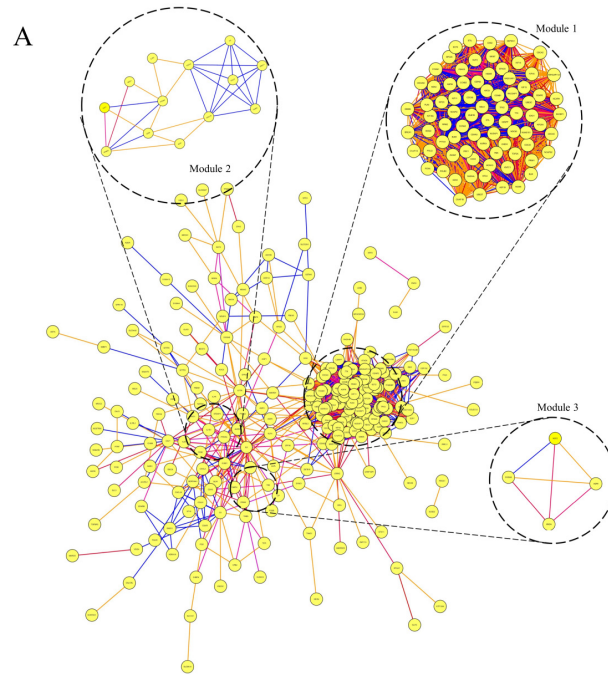


Figure 2: Top 3 modules from the protein-protein interaction network.

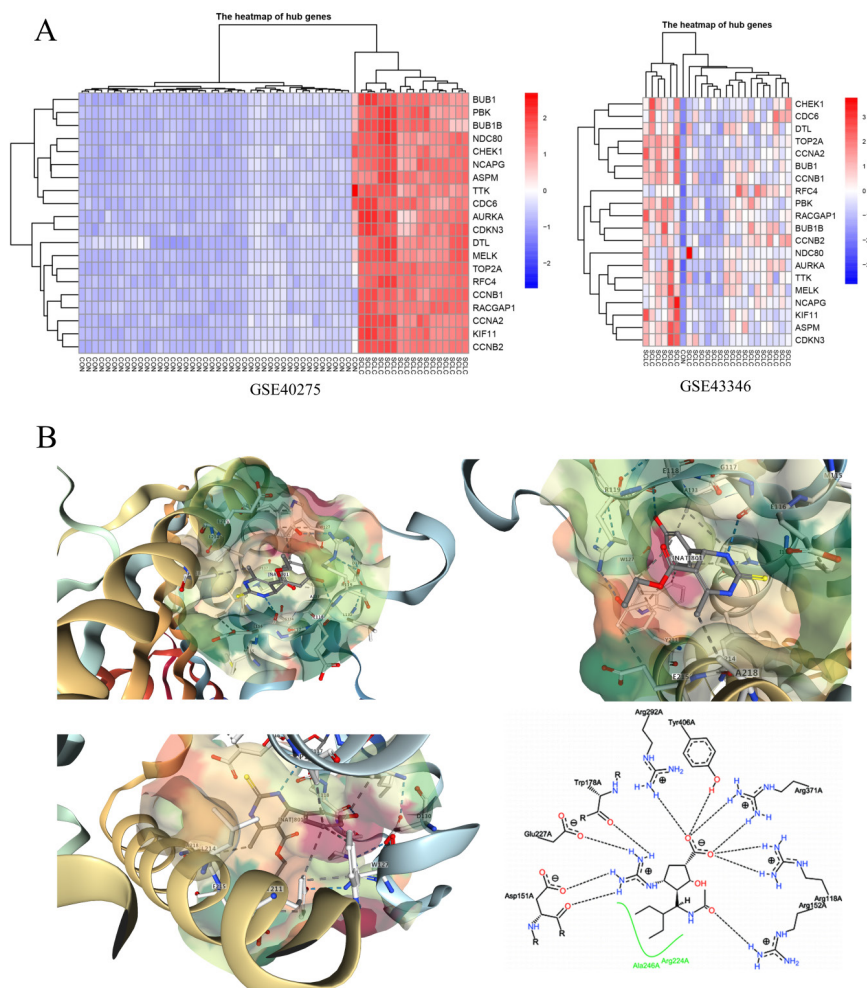
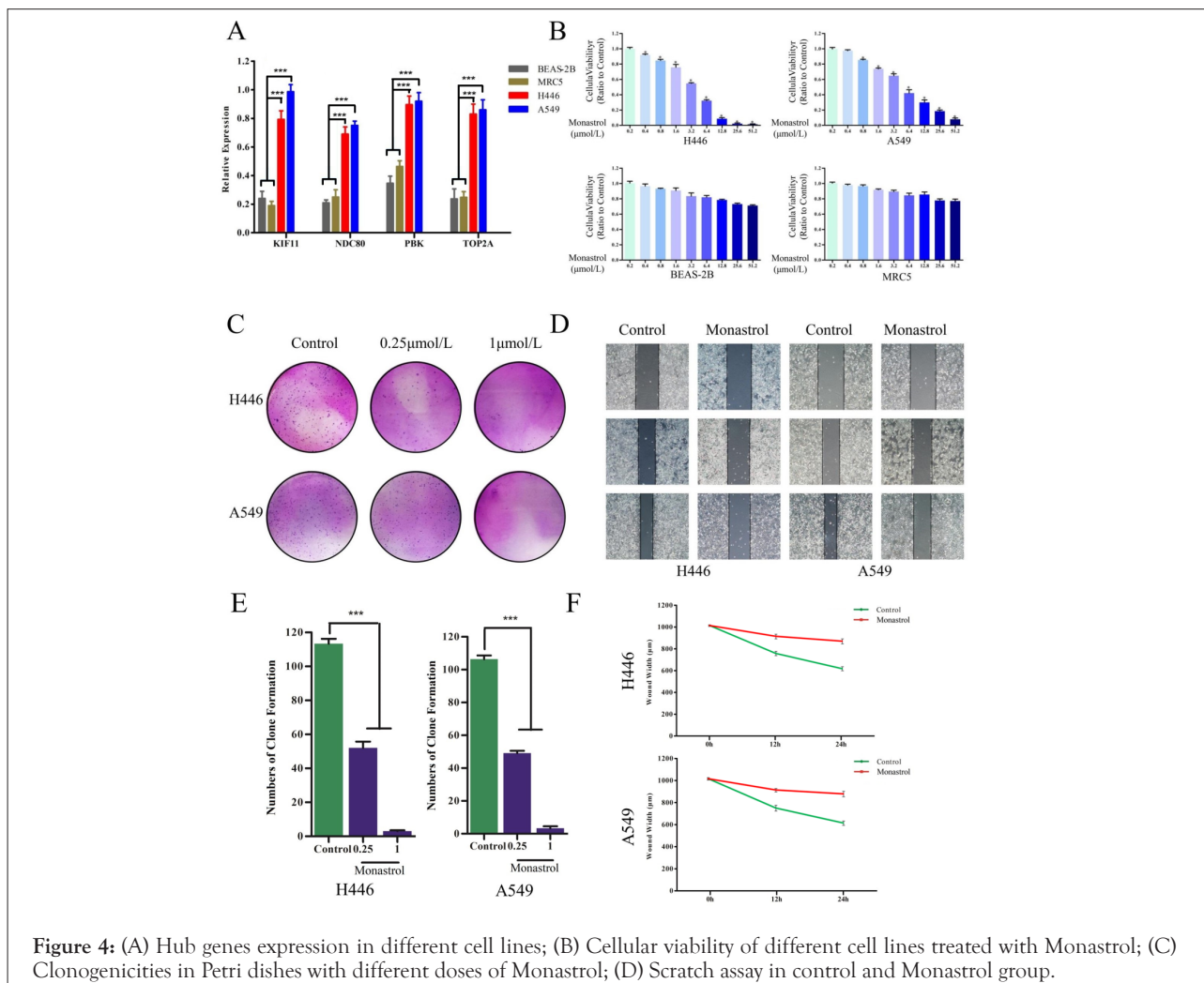


Figure 3: (A) Hub genes expression heat map of GSE40275 and GSE43346; (B) Binding of Monastrol to *KIF11* protein.

Table 3: The functional annotation and enrichment of modules genes.

The functional annotation and enrichment of modules genes						
Module	Term	Count	P value	FDR	Genes	
Module 1	GO:0051301 ~ Cell division	74	6.45E-15	7.65E-12	KIF23, STIL, PRC1, EZH2, KNTC1, TTK, AURKA, PTTG1, MCM10, KIF2C, CDCA8, TOP2A, CCNA2, CDCA5, KIF14, CDC6, DTL, KIF15, TPX2, NUSAP1, DEPDC1, MCM2, PBK, UBE2C, ECT2, MCM6, RFC5, RFC3, RFC4, SPAG5, RRM2, ZWINT, BUB1B, MELK, SHCBP1, KIF4A, BLM, NEK2, FOXM1, KIAA0101, CHEK1, CEP55, HMMR, SPC25, NCAPH, POLE2, NCAPG2, NCAPG, BUB1, FBXO5, ASF1B, POLQ, EXO1, RAD51A1, MKI67, GMNN, KIF18A, NUF2, CENPF, NDC80, CENPE, CDC20, CDC25C, CENPK, RACGAP1, CDKN3, RAD54L, BRCA1, CCNB1, PLK4, CCNB2, PCNA, CKS2, KIF20A	
		33	3.32E-15	2.00E-29	NEK2, KNTC1, AURKA, PTTG1, SPC25, KIF2C, CDCA8, NCAPH, CDCA7, NCAPG2, NCAPG, CDCA2, BUB1, FBXO5, CCNA2, CDCA5, KIF14, CDC6, KIF11, TPX2, NUF2, CENPF, NDC80, CENPE, CDC20, CDC25C, UBE2C, CCNB1, CCNB2, SPAG5, ZWINT, CKS2, BUB1B	
	hsa04110: Cell cycle	14	4.74E-15	3.87E-12	CDC6, TTK, CDC20, CHEK1, PTTG1, MCM2, CDC25C, MCM6, CCNB1, CCNB2, PCNA, BUB1, BUB1B, CCNA2	
Module 2	GO:0006954 ~ Inflammatory response	6	3.97E-06	0.0054503	C5AR1, OLR1, PTGS2, C3, CCL21, CXCL2	
	GO:0005886 ~ Plasma membrane	8	8.01E-03	7.5487027	CAVI, IL1R1, CD36, C5AR1, OLR1, C3, CXCL16, GNG11	
	hsa04062: Chemokine signaling pathway	4	2.73E-03	2.697201	CCL21, CXCL16, CXCL2, GNG11	
Module 3	GO:0006968 ~ Cellular defense response	2	1.10E-02	10.662027	NCF2, MND4	



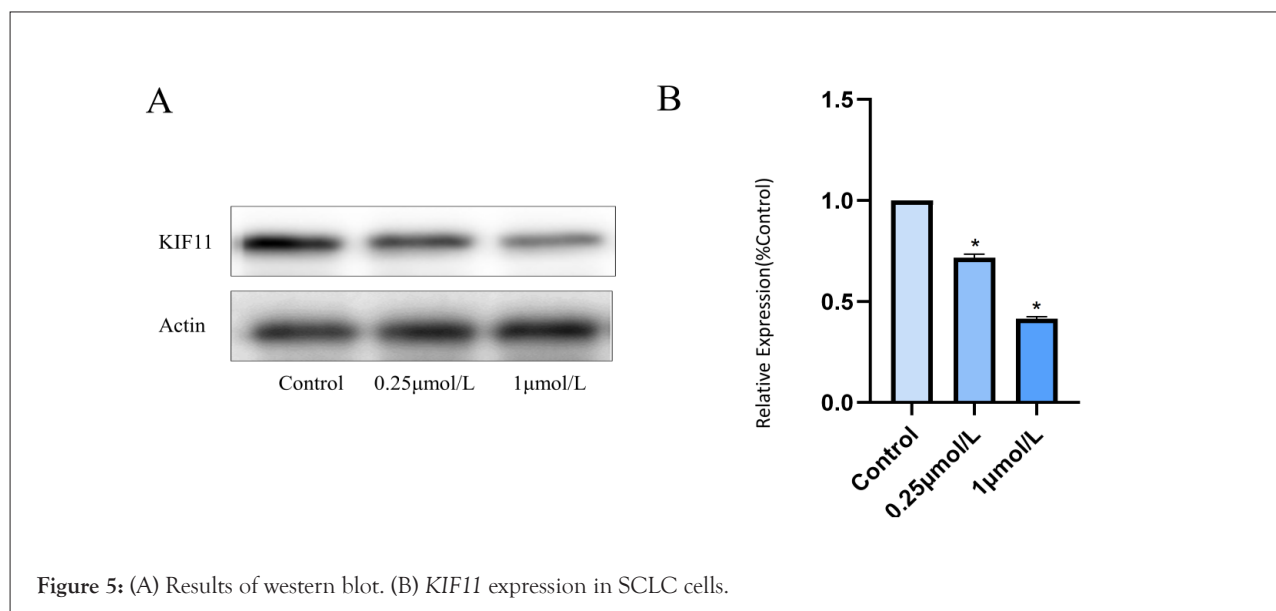


Figure 5: (A) Results of western blot. (B) *KIF11* expression in SCLC cells.

DISCUSSION

SCLC is often diagnosed in an advanced stage, which is a highly aggressive malignancy associated with early metastasis, rapid progression, and poor survival. First-line chemotherapy provides good response rates in advanced disease, but SCLC often relapses, progression-free and overall survival is limited. Few related genes and molecular pathways have been studied by previous researchers, there is an urgent need for comprehensive analysis regarding SCLC [8,9]. And clinical diagnosis, treatment, and prognosis would be significantly improved if the appropriate targets are identified. Our study used bioinformatics analysis techniques combined with a complicated and refined algorithm to identify key genes and pathways, which could provide potential targets for SCLC diagnosis and treatment. And screening anti-SCLC drugs based on targets to improve clinical treatment.

GSE40275 and GSE43346 datasets were downloaded, and then we screened normal tissues and SCLC tissues samples from them, also identified the DEG's between normal tissues and SCLC tissues. Results showed that there were 305 DEGs, 129 up-regulated and 176 down-regulated. The functions and corresponding signaling pathways of DEG's were investigated by GO and KEGG analysis. The cell division and sister chromatid cohesion biological process are up-regulated observably, at the same time, the ratios of nucleus-related components are up-regulated obviously. These changes may favor the preparation for DNA replication and promote the self-duplication of SCLC cells. The infinite proliferation of tumor cells is actually the abnormality of cell division and might be the result of Insensitivity to Antigrowth Signals. The signal pathway of Oocyte meiosis abnormal activation suggests that there is a difference in the incidence of SCLC between men and women. Meanwhile, the formation of neovascularization is closely related to the development of tumors, Fanconi anemia pathway exceeding activation plays an important role in the occurrence and development of SCLC. The positive regulation of vasoconstriction is down-regulated, and the continuous supply of blood flow is related to the need for adequate blood supply for the growth of tumor tissue. The changes in extracellular membrane components regulate the recognition and signal transmission between tumor cells and promote the migration of tumor cells at the same time. At

the same time, the scavenger receptor activity is suppressed which may cause the body unable to recognize and remove abnormal cells, leading to carcinogenesis, and then SCLC occurs. These results further explain the tumor formation mechanism of SCLC and also provide novel ideas for further study of SCLC in the future.

PPI network of DEG's was constructed using the STRING database and Cytoscape. Three hub genes (*KIF11*, *NDC80*, and *PBK*) were identified as driver genes closely related to SCLC development and they had never been reported related to SCLC in previous studies. *KIF11*, kinesin family member 11, located in Chr10q23.33, encodes a motor protein that is known to be involved in spindle assembly, control of mitotic spindle structure, and chromosome behavior during mitosis [10,11]. The function of this protein includes chromosome positioning, centrosome separation, and establishing a bipolar spindle during cell mitosis. Kinesin motor domains couple cycles of ATP hydrolysis to cycles of microtubule binding and conformational changes that result in directional force and movement on microtubules [12]. Meanwhile, *KIF11* dephosphorylation can lead to a mitotic exit, and the expression level of this gene is low in normal lung tissue [13,14]. In SCLC cells, overexpression of this gene may lead to a rise in phosphorylated Erk1/2 levels, and promote bipolar spindle assembly and chromosome segregation [15-17]. And this gene also plays a role in DNA repair, gives assistance for some protein transport from the trans-Golgi network to the cell surface, and contributes to mitotic spindle checkpoint activation and Tat-mediated apoptosis in CD4-positive T-lymphocytes, which may boost the progress of small cell lung cancer development. Given these circumstances, *KIF11* might be a potential microtubule-related target for proliferating SCLC cells [18-21]. It prompted us to hypothesize that Monastrol, a potent and cell-permeable inhibitor that targeted *KIF11* with an IC50 value of 14 μM, which causes aberrant interactions with the microtubule, and reversals at the ATP hydrolysis step, might have anti-SCLC therapeutic effects [22-24]. And it had also been verified by the following assays in this study. The drug in protein binding structure 1X88 was downloaded in the PDB dataset (Protein Data Bank, <http://www.rcsb.org/>), and shown in Figure 3B.

NDC80, kinetochore complex component, located in Chr18p11.32, encoded protein consists of an N-terminal microtubule-binding domain and a C-terminal coiled-coiled domain that interacts with

other components of *NDC80* kinetochore complex, which directly modulates microtubule dynamics [25]. This protein functions to organize and stabilize microtubule-kinetochore interactions and is required for proper chromosome segregation. Aurora A kinase phosphorylates *NDC80* to regulate metaphase kinetochore-microtubule dynamics [26] and Aurora B-*NDC80*-Mps1 signaling axis is governing accurate chromosome segregation in mitosis [27]. Overproduction of *NDC80* in cancer cells unfavorably absorbs protein interactors through the internal loop domain and leads to a change in the equilibrium of microtubule-associated proteins [28]. *NDC80*'s interaction with either growing or shrinking microtubule ends such as differentially regulating mammalian kinetochore coupling to polymerizing and depolymerizing microtubules can be tuned by the phosphorylation state of its tail [29,30]. N-terminus-modified *NDC80* can suppress tumor growth by interfering with kinetochore-microtubule dynamics [31]. Our study showed that this gene, which was the core of the interaction with multiple genes, had a pivotal position in SCLC tissues. The expression of this gene was abnormally regulated because *NDC80* was a driver gene of SCLC, we hypothesized its abnormal activation would promote the initiation of SCLC, it might play an important role during SCLC development and it might be a biomarker in the early diagnosis of SCLC. Accordingly, *NDC80* could be considered an important therapeutic target for SCLC.

PBK, PDZ binding kinase, this gene locates at Chr8p21.1 and encodes a serine/threonine protein kinase related to the dual specific Mitogen-Activated Protein Kinase (MAPK) family. This kinase can increase the rate of mitosis and expands malignant T cells [32]. FoxM1-regulated *PBK* exerts oncogenic activities *via* the activation of the beta-Catenin pathway [33]. CDK1-mediated mitotic phosphorylation of *PBK* is involved in cytokinesis and inhibits its oncogenic activity [34]. *PBK* promotes lung cancer resistance to EGFR tyrosine kinase inhibitors by phosphorylating and activating c-Jun [35]. *PBK* mediates promyelocyte proliferation *via* Nrf2-regulated cell cycle progression and apoptosis [36]. *TOPK/PBK* promotes cell migration *via* modulation of the PI3K/PTEN/AKT pathway and is associated with poor prognosis in lung cancer [37]. Increased levels of *PBK* may contribute to tumor cell development and progression through suppression of p53 function and consequent reductions in the cell-cycle regulatory proteins such as p21 [38]. *PBK* augments tumor cell growth following a transient appearance in different types of progenitor cells *in vivo* as reported [39]. Overexpression of this gene has been implicated in tumorigenesis. Over expression of *PBK* contributes to tumor development and poor outcome of SCLC [40]. *PBK* might play a pivotal role in SCLC invasion and metastasis [41]. Our research confirms that the expression of this gene was abnormal regulated and it is a core driver gene of SCLC.

The effects of Monastrol were evaluated in the present study with MTT assay, colony-forming assay, and scratch assay *in vitro*. In MTT assay, the cellular viability (ratio to control) in H446 and A549 cell lines was revealed dose-dependent decreased when treated with Monastrol. In the colony-forming assay, the numbers and size of clonogenicities in the Monastrol group were significantly less than in the control group, which was consistent with the results that Monastrol can reduce the proliferation of SCLC cells. In scratch assay, the wound widths in the control group decreased sharply along with time and were smaller than that in Monastrol group after 48 h significantly. That implied that Monastrol strongly

inhibited the migration of SCLC cells. All these results suggest that Monastrol has the potential effect on treating SCLC, which is worthy of further study.

CONCLUSION

Our study screened out the DEG's and key pathways in SCLC. The DEG's identified in this study provided comprehensive insight into the molecular mechanism of SCLC pathogenesis. Three hub genes: *KIF11*, *NDC80*, and *PBK* were aberrantly expressed and could be potentially applied as diagnostic biomarkers, therapeutic targets, and prognostic biomarkers. Meanwhile, Monastrol, a potent inhibitor of *KIF11*, suppressed the proliferation and migration of SCLC cells and was a promising drug in the treatment of SCLC patients.

FUNDING

We thank the foundation of the Henan Medical Science and Technology Public Relations Project (LHGJ202105534) of the First People's Hospital of Xinxiang for financial support of this work.

REFERENCES

1. Stumpf C, Kaemmerer D, Neubauer E, Sanger J, Schulz S, Lupp A. Somatostatin and CXCR4 expression patterns in adenocarcinoma and squamous cell carcinoma of the lung relative to small cell lung cancer. *J Cancer Res Clin Oncol*. 2018;144(10):1921-1932.
2. Zhao H, Ren D, Liu H, Chen J. Comparison and discussion of the treatment guidelines for small cell lung cancer. *J Thorac Cancer*. 2018;9(7):769-774.
3. Bunn PA, Minna JD, Augustyn A, Gazdar AF, Ouadah Y, Krasnow MA, et al., Small cell lung cancer: Can recent advances in biology and molecular biology be translated into improved outcomes? *J Thorac Cancer*. 2016;11(4):453-474.
4. Byers LA, Rudin CM. Small cell lung cancer: Where do we go from here? *Cancer*. 2015;121(5):664-672.
5. Kalemkerian GP, Akerley W, Bogner P, Borghaei H, Chow LQ, Downey RJ, et al. Small cell lung cancer. *J Natl Compr Canc Netw*. 2013;11(1):78-98.
6. Pillai RN, Owonikoko TK. Small cell lung cancer: therapies and targets. *Seminars in Oncology*. 2014;41(1):133-142.
7. Dang Wei, Bian Rui, Fan Qingquan. *KIF11* promotes cell proliferation *via* ERBB2/PI3K/AKT signaling pathway in gallbladder cancer. *Int J Biol Sci*. 2021;17(2):514-526.
8. Hendriks LEL, Menis J, Reck M. Prospects of targeted and immune therapies in SCLC. *Expert Rev Anticancer Ther*. 2018:1-17.
9. Wang Z, Fu S, Zhao J, Zhao W, Shen Z, Wang D, et al. Transbronchoscopic patient biopsy-derived xenografts as a preclinical model to explore chemorefractory-associated pathways and biomarkers for small-cell lung cancer. *Cancer Lett*. 2019;440-441:180-188.
10. Duan Y, Huo D, Gao J, Wu H, Ye Z, Liu Z, et al. Ubiquitin ligase RNF20/40 facilitates spindle assembly and promotes breast carcinogenesis through stabilizing motor protein Eg5. *Nat Commun*. 2016;7:12648.
11. He J, Zhang Z, Ouyang M, Yang F, Hao H, Lamb KL, et al. PTEN regulates EG5 to control spindle architecture and chromosome congression during mitosis. *Nat Commun*. 2016;7:12355.
12. Scarabelli G, Grant BJ. Kinesin-5 allosteric inhibitors uncouple the dynamics of nucleotide, microtubule, and neck-linker binding sites. *Biophysical Journal*. 2014;107(9):2204-2213.

13. Liu Y, Zhang Z, Liang H, Zhao X, Liang L, Wang G, et al. Protein phosphatase 2A (PP2A) regulates Eg5 to control mitotic progression. *Scientific Reports*. 2017;7(1):1630.
14. Fagerberg L, Hallstrom BM, Oksvold P, Kampf C, Djureinovic D, Odeberg J, et al. Analysis of the human tissue-specific expression by genome-wide integration of transcriptomics and antibody-based proteomics. *Mol Cell Proteomics*. 2014;13(2):397-406.
15. Imai T, Oue N, Nishioka M, Mukai S, Oshima T, Sakamoto N, et al. Overexpression of *KIF11* in Gastric Cancer with Intestinal Mucin Phenotype. *Pathobiology*. 2017;84(1):16-24.
16. Van Heesbeen RG, Tanenbaum ME, Medema RH. Balanced activity of three mitotic motors is required for bipolar spindle assembly and chromosome segregation. *Cell Rep*. 2014;8(4):948-956.
17. Gayek AS, Ohi R. Kinetochores-microtubule stability governs the metaphase requirement for Eg5. *Mol Biol Cell*. 2014;25(13):2051-2060.
18. Tan LJ, Saijo M, Kuraoka I, Narita T, Takahata C, Iwai S, et al. Xeroderma pigmentosum group F protein binds to Eg5 and is required for proper mitosis: Implications for XP-F and XFE. *Genes Cells*. 2012;17(3):173-185.
19. Wakana Y, Villeneuve J, van Galen J, Cruz-Garcia D, Tagaya M, Malhotra V. Kinesin-5/Eg5 is important for transport of CARTS from the trans-Golgi network to the cell surface. *The Journal of Cell Biology*. 2013;202(2):241-250.
20. Liu M, Li D, Sun L, Chen J, Sun X, Zhang L, Huo L, Zhou J. Modulation of Eg5 activity contributes to mitotic spindle checkpoint activation and Tat-mediated apoptosis in CD4-positive T-lymphocytes. *J Pathol*. 2014;233(2):138-147.
21. Hayashi N, Koller E, Fazli L, Gleave ME. Effects of Eg5 knockdown on human prostate cancer xenograft growth and chemosensitivity. *Prostate*. 2008;68(12):1283-1295.
22. Rose AS, Bradley AR, Valasatava Y, Duarte JM, Prlic A, Rose PW. NGL viewer: Web-based molecular graphics for large complexes. *Bioinformatics*. (Oxford, England). 2018;34(21):3755-3758.
23. Cochran JC, Gatial JE, 3rd, Kapoor TM, Gilbert SP. Monastrol inhibition of the mitotic kinesin Eg5. *J Biol Chem*. 2005;280(13):12658-12667.
24. Garcia-Saez I, DeBonis S, Lopez R, Trucco F, Rousseau B, Thuery P, et al. Structure of human Eg5 in complex with a new monastrol-based inhibitor bound in the R configuration. *J Biol Chem*. 2007;282(13):9740-9747.
25. Umbreit NT, Gestaut DR, Tien JF, Vollmar BS, Gonen T, Asbury CL, et al. The Ndc80 kinetochore complex directly modulates microtubule dynamics. *Proc Natl Acad Sci USA*. 2012;109(40):16113-16118.
26. DeLuca KF, Meppelink A. Aurora A kinase phosphorylates Hec1 to regulate metaphase kinetochore-microtubule dynamics. *J Cell Biol*. 2018;217(1):163-177.
27. Zhu T, Dou Z, Qin B, Jin C, Wang X, Xu L, et al. Phosphorylation of microtubule-binding protein Hec1 by mitotic kinase Aurora B specifies spindle checkpoint kinase Mps1 signaling at the kinetochore. *J Bio Chem*. 2013;288(50):36149-36159.
28. Tang NH, Toda T. MAPPING the Ndc80 loop in cancer: A possible link between Ndc80/Hec1 overproduction and cancer formation. *BioEssays*. 2015;37(3):248-256.
29. Alushin GM, Musinipally V, Matson D, Tooley J, Stukenberg PT, Nogales E. Multimodal microtubule binding by the Ndc80 kinetochore complex. *Nat Struct Mol Biol*. 2012;19(11):1161-1167.
30. Long AF, Udy DB, Dumont S. Hec1 Tail Phosphorylation Differentially Regulates Mammalian Kinetochore Coupling to Polymerizing and Depolymerizing Microtubules. *Curr Biol*. 2017;27(11):1692-1699.
31. Orticello M, Fiore M, Totta P, Desideri M, Barisic M, Passeri D, et al. N-terminus-modified Hec1 suppresses tumour growth by interfering with kinetochore-microtubule dynamics. *Oncogene*. 2015;34(25):3325-3335.
32. Ishikawa C, Senba M, Mori N. Mitotic kinase PBK/TOPK as a therapeutic target for adult T-cell leukemia/lymphoma. *Int J Oncol*. 2018;53(2):801-814.
33. Yang YF, Pan YH, Cao Y, Fu J, Yang X, Zhang MF, et al. PDZ binding kinase, regulated by FoxM1, enhances malignant phenotype via activation of beta-Catenin signaling in hepatocellular carcinoma. *Oncotarget*. 2017;8(29):47195-47205.
34. Stauffer S, Zeng Y, Zhou J, Chen X, Chen Y, Dong J. CDK1-mediated mitotic phosphorylation of PBK is involved in cytokinesis and inhibits its oncogenic activity. *Cell signal*. 2017;39:74-83.
35. Li Y, Yang Z, Li W, Xu S, Wang T, Wang T, et al. TOPK promotes lung cancer resistance to EGFR tyrosine kinase inhibitors by phosphorylating and activating c-Jun. *Oncotarget*. 2016;7(6):6748-6764.
36. Liu Y, Liu H, Cao H, Song B, Zhang W, Zhang W. PBK/TOPK mediates promyelocyte proliferation via Nrf2-regulated cell cycle progression and apoptosis. *Oncol Rep*. 2015;34(6):3288-3296.
37. Shih MC, Chen JY, Wu YC, Jan YH, Yang BM, Lu PJ, et al. TOPK/PBK promotes cell migration via modulation of the PI3K/PTEN/AKT pathway and is associated with poor prognosis in lung cancer. *Oncogene*. 2012;31(19):2389-2400.
38. Hu F, Gartenhaus RB, Eichberg D, Liu Z, Fang HB, Rapoport AP. PBK/TOPK interacts with the DBD domain of tumor suppressor p53 and modulates expression of transcriptional targets including p21. *Oncogene*. 2010;29(40):5464-5474.
39. Nandi AK, Ford T, Fleksher D, Neuman B, Rapoport AP. Attenuation of DNA damage checkpoint by PBK, a novel mitotic kinase, involves protein-protein interaction with tumor suppressor p53. *Biochem Biophys Res Commun*. 2007;358(1):181-188.
40. Ohashi T, Komatsu S, Ichikawa D, Miyamae M, Okajima W, Imamura T, et al. Overexpression of PBK/TOPK contributes to tumor development and poor outcome of esophageal squamous cell carcinoma. *Anticancer Res*. 2016;36(12):6457-6466.
41. Seol MA, Park JH, Jeong JH, Lyu J, Han SY, Oh SM. Role of TOPK in lipopolysaccharide-induced breast cancer cell migration and invasion. *Oncotarget*. 2017;8(25):40190-40203.